ELSEVIER

Journal of Alloys and Compounds 281 (1998) 211–221

Journal of ALLOYS AND COMPOUNDS

Induced helices, tetrahedrons and spirals in yellow InCl

W.J.A. Maaskant*

Leiden Institute of Chemistry, Gorlaeus Laboratories, P.O. Box 9502, 2300 RA Leiden, The Netherlands

Received 22 July 1998

Abstract

The structure of yellow InCl is explained. The cubic cell contains 20 trigonally and 12 digonally distorted $InCl_6$-octahedra, due to the $(5s)^2$-outer electron configuration of In^+. To a good approximation the structure can be seen as distorted rocksalt, due to three equally strong lattice modes. The distortions of the local octahedra, of various symmetry-type, can be calculated from the structure, derived from available XRD-data. It is possible from these to deduce bilinear forms, which express chirality, tetrahedron forming and spiral forming. Chirality is especially interesting, since there is an optical analogue and one of the expressions for chirality resembles the rotational strength as described by Condon for optical rotation. The other form of chirality goes beyond the Condon approximation and arises since the size of these octahedra is about 1/3 of the wave length of the helices. The three lattice modes induce a number of anti-ferrodistortive distributions of helices, tetrahedrons and spirals. In addition, there is also one ferrodistortive component for chirality and one for tetrahedron forming. © 1998 Elsevier Science S.A. All rights reserved.

Keywords: Lone pairs; Pseudo-Jahn–Teller effect; Chirality

1. Introduction

The monopositive ion In^+ has the outer electronic structure of $(5s)^2$. In InCl it exhibits stereochemical activity of the lone pair of electrons in several ways. InCl occurs in a yellow and a red form. The red crystals have the so-called β-TlI structure, which occurs more often for A^+B^--compounds where A^+ has a lone electron pair. The structure of yellow InCl is unique in the sense, that no other compound with this crystal structure is known. Yellow InCl is stable below 390 K. We will discuss in this paper only yellow InCl, which will be denoted as InCl.

The crystal structure of (yellow) InCl has been determined by XRD for the first term by Van den Berg [1,2]; the structure has been redetermined by Van der Vorst, Verschoor and Maaskant [3]. Van den Berg tried to rationalize the observed structure by assuming metal–metal bonding. However, Van der Vorst and Maaskant [4] argued that both in yellow and red InCl stereochemically active lone pairs on the In^+-ions are present.

The important contribution from the Jahn–Teller point of view is from Öpik and Pryce [6] mainly for the description of the $T\otimes(\epsilon_g+t_{2g})$ Jahn–Teller effect (JTE) for an electron in an orbital T-state. They also mention the possibility of mixing of electronic 2s and 2p states for one electron in an excited F-center by means of t_{1u} vibrations, which is called a pseudo Jahn–Teller effect (PJTE). Ham [7] studied these F-centers more extensively and discussed already trigonally and tetragonally deformed octahedra. Pearson [8] introduced the concept in another field, calling it second order Jahn–Teller effect. Maaskant and Bersuker [9] reformulated the theory for one and for two electrons. A pseudo Jahn–Teller effect occurs through the t_{1u}-modes, which couple the A_{1g} ground state and the T_{1u}-excited state. Since the T_{1u}-state is Jahn–Teller active, one can speak of a combined PJTE and JTE. Important results are that for a single octahedron with a stereochemical lone pair on the central ion four forms can be derived: An undistorted octahedron, a 'trigonal' one, a 'tetragonal' one and an 'intermediate' form. For isolated octahedra the (linear) theory predicts that in the case of a PJTE the 'intermediate' form has an energy in between the 'trigonal' and the 'tetragonal' species [7,9]. However, from these theories it cannot be deduced whether the 'trigonal' or the 'tetragonal' variant is the most stable one. Maaskant [10] has studied the local octahedra in yellow and in red InCl earlier. From the occurrence of the 'trigonal' species and the total absence of the 'tetragonal' form in the crystal structure, it can be concluded that in InCl the 'trigonal' variant is the most stable one. However, there appears to be an additional anharmonic energy term in the 'inter-

*Corresponding author. Tel.: +31-71-527-4214; fax: +31-71-527-4537; e-mail: maaskant@chem.leidenuniv.nl

0925-8388/98/$ – see front matter © 1998 Elsevier Science S.A. All rights reserved.
PII: S0925-8388(98)00788-9

mediate' species (in this paper called the 'digonal' form). This anharmonicity will be shown to be essential for the existence of this crystal structure.

The space group of InCl is $P2_13$ ($Z=32$). It is a subgroup of $Fm\bar{3}m$, the space group of rocksalt (also referred to as the B1 structure). The symmetry lowering is a factor 128, obtained by an increase of the cell volume by a factor of 32 (one should consider the primitive cell of rocksalt) and a factor of four for the lowering of the point group of the crystal from O_h to T. The 32 In^+ ions are placed in two twelve-fold and two fourfold positions. The fourfold positions are on threefold rotation axes. The same applies to the Cl^--ions. These sites have been numbered 1 to 4 by Van der Vorst et al. [4]. It turns out that the $InCl_6$-complexes (type 3 and 4) with the fourfold positions are trigonal. This is almost so for the twelve-fold position type 2. The type 1 $InCl_6$ can better be described as digonal. Fig. 1 gives an impression of the trigonally and of the digonally distorted octahedra. More exact drawings from the $ClIn_6$-octahedra also have been published by Van der Vorst and Maaskant, [4]. It is not difficult to derive the actual displacements from the NaCl-positions. Although the crystal structure determinations have been reported in the scheme of the International Tables, Van der Vorst [5] gave already the amplitudes of the observed lattice symmetry modes, referred to the rocksalt structure.

Although no phase transition to the rocksalt structure has been found, it is enlightening to discuss the conditions for a second order phase transition according to Landau [11,12] or Landau and Lifshitz [13]. For the case of a continuous or second order phase transition in solids, Landau and Lifshitz showed that an expansion of the free energy in terms of the relevant order parameter should be possible. There are four conditions to be fulfilled. These can be investigated by group theory (mostly solid state group theory). When a subgroup–group relationship exists between two phases of a compound, it is possible to investigate these conditions and determine whether the transition is of second order, or for what reason this is not to be expected. Notice that the first condition has been satisfied: The space group of InCl is a subgroup of the space group of rocksalt.

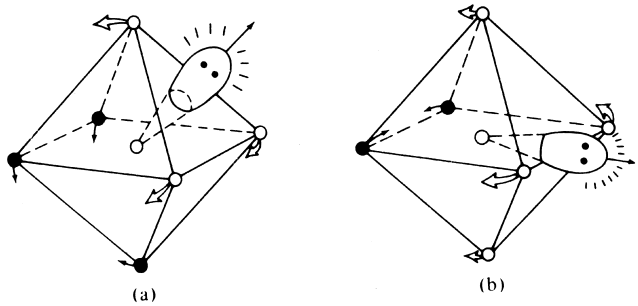

Fig. 1. Trigonally (a) and digonally (b) distorted octahedrons due to a stereochemically active lone pair.

Table 1
Deviations in yellow InCl from the idealized B1 positions given as fractions of the cubic cell parameter of InCl

Ion	x_0	y_0	z_0	δ_x	δ_y	δ_z
In(1)	$\frac{1}{4}$	$\frac{1}{4}$	0	−0.0013	−0.0302	−0.0288
In(2)	$\frac{3}{4}$	$\frac{3}{4}$	0	0.0027	0.0281	0.0295
In(3)	0	0	0	0.0302	0.0302	0.0302
In(4)	$\frac{1}{2}$	$\frac{1}{2}$	$\frac{1}{2}$	−0.0327	−0.0327	−0.0327
Cl(1)	$\frac{1}{4}$	0	0	0.0505	−0.0504	0.0005
Cl(2)	$\frac{3}{4}$	0	0	0.0498	0.0549	−0.0110
Cl(3)	$\frac{1}{4}$	$\frac{1}{4}$	$\frac{1}{4}$	−0.0439	−0.0439	−0.0439
Cl(4)	$\frac{3}{4}$	$\frac{3}{4}$	$\frac{3}{4}$	0.0486	0.0486	0.0486

This paper is a simplified discussion of a paper by us [14]. The proofs of formulae by means of solid state group theory have been omitted. For clarification only a limited amount of group theory for point groups will be used, as is given by e.g. Cotton [15].

2. The deformations

Table 1 expresses the experimental distortions from the B1(rocksalt) structure. The B1 positions, expressed in the cell of InCl, are given in the columns headed by x_0, y_0, z_0. The deviations (δ_x, δ_y, δ_z) are, in absolute sense, an order of magnitude smaller than the rocksalt values, giving further evidence of the subgroup–group relationship between yellow InCl and the B1 structure.

Table 2 gives the experimental symmetry coordinates. These have for the first time been calculated by Van der Vorst (1981) [5], but in [14] we give slightly different normalized lattice modes. The primed symbols denote the In ions, while the unprimed symbols denote the Cl ions. The precision of these numbers is the same as that for the crystal structure determination. Obviously some of these symmetry coordinates are large and others very small. We have therefore made an approximation, the 'geometric' approximation. In Table 3 we list the parameters of this approximation. There are two circularly polarized waves: Those with the d- and d'-parameters, the Δ-waves, and those with the w- and w'-parameters, the W-waves. The

Table 2
Experimental symmetry coordinates

$d'_1=0.0197$	$s'_1=-0.0001$	$d_1=0.0272$	$s_1=-0.0001$
$d'_2=-0.0191$	$s'_2=-0.0014$	$d_2=-0.0248$	$s_2=0.0028$
$w'_1=0.0188$	$s'_3=-0.0252$	$w_1=-0.0342$	$s_3=-0.0456$
$w'_2=0.0166$	$l'_1=-0.0002$	$w_2=0.0318$	$l_2=0.0002$

Table 3
Symmetry coordinates for the 'geometric' approximation

$d'_1=0.0184$	$s'_1=0.0000$	$d_1=0.0300$	$s_1=0.0000$
$d'_2=-0.0184$	$s'_2=0.0000$	$d_2=-0.0300$	$s_2=0.0000$
$w'_1=0.0184$	$s'_3=-0.0260$	$w_1=-0.0300$	$s_3=-0.0425$
$w'_2=0.0184$	$l'_1=0.0000$	$w_2=0.0300$	$l_2=0.0000$

Table 4
The coordinates arising from the 'geometric' approximation and the deviations of the observed coordinates (the last three columns)

Ion	x_0	y_0	z_0	δ_x	δ_y	δ_z	u_x	u_y	u_z
In(1)	$\frac{1}{4}$	$\frac{1}{4}$	0	0.0000	−0.0301	−0.0301	−0.0013	−0.0001	0.0013
In(2)	$\frac{3}{4}$	$\frac{3}{4}$	0	0.0000	0.0301	0.0301	0.0027	−0.0020	−0.0006
In(3)	0	0	0	0.0301	0.0301	0.0301	0.0001	0.0001	0.0001
In(4)	$\frac{1}{2}$	$\frac{1}{2}$	$\frac{1}{2}$	−0.0301	−0.0301	−0.0301	−0.0026	−0.0026	−0.0026
Cl(1)	$\frac{1}{4}$	0	0	0.0491	−0.0491	0.0000	0.0014	−0.0013	0.0000
Cl(2)	$\frac{3}{4}$	0	0	0.0491	0.0491	0.0000	0.0007	0.0058	−0.0115
Cl(3)	$\frac{1}{4}$	$\frac{1}{4}$	$\frac{1}{4}$	−0.0491	−0.0491	−0.0491	0.0052	0.0052	0.0052
Cl(4)	$\frac{3}{4}$	$\frac{3}{4}$	$\frac{3}{4}$	0.0486	0.0486	0.0486	−0.0005	−0.0005	−0.0005

one with the s_3- and the s_3'-parameters, the Σ_4 mode is single and the absolute values of its parameters are $\sqrt{2}$ larger than the former parameters. The smaller coordinates are put equal to zero. In this way we have introduced an approximation with three distortion modes of equal strength. That this is a reasonable approximation is seen in Table 4, where the remaining deviations are shown to be an order of magnitude smaller than the 'geometric approximation'.

Here arises a discrepancy with the second Landau condition for continuous phase transitions. According to Landau and Lifshitz only one symmetry mode of a certain irreducible representation of the space group can be involved. And we have three modes of different symmetry types. The idea behind this second condition is, that modes of different symmetries are expected to have different constants and therefore also different phase transition points. However, in the case of InCl this does not pose any problem, since there is no phase transition. In addition we will show in Section 4 that these modes are nearly degenerate. Though this degeneracy cannot be proven exactly, the choice of the equal amplitudes for these modes appears to be the correct starting point for the discussion.

Table 6
The positions of the ions chosen in Table 5 in fractions of the InCl cell parameter

	In(1)	In(2)	In(3)	In(4)	Cl(1)	Cl(2)	Cl(3)	Cl(4)
x	$\frac{1}{4}$	$\frac{3}{4}$	0	$\frac{1}{2}$	$\frac{1}{2}$	$\frac{1}{2}$	$\frac{1}{4}$	$\frac{3}{4}$
y	0	0	0	$\frac{1}{2}$	0	0	$\frac{1}{4}$	$\frac{3}{4}$
z	$\frac{3}{4}$	$\frac{1}{4}$	0	$\frac{1}{2}$	$\frac{3}{4}$	$\frac{1}{4}$	$\frac{1}{4}$	$\frac{3}{4}$

Finally in Table 5 Table 6 the local distortion modes for all types of octahedral environment are given. These have been calculated with the symmetry modes defined in Appendix A. One sees a lot of equal numbers. This arises because of the 'geometric approximation' but also because the modes are not independent. From Table 1 or Table 2 there appear to be only 16 independent parameters, which have reduced to 2 in Table 3. What is surprising, however, is the complexity which arises in these distortions. With a

Table 5
Idealized octahedral symmetry coordinates given as fractions of the cell parameter of InCl$\times 10^4$. The ideal coordinates for the four In sites the four Cl sites are given in Table 6

	In(1)	In(2)	In(3)	In(4)	Cl(1)	Cl(2)	Cl(3)	Cl(4)
$q(a_{1g})$	0	0	0	0	0	0	0	0
$q(e_{g\theta})$	0	0	0	0	0	0	0	0
$q(e_{g\epsilon})$	0	0	0	0	0	0	0	0
$q(t_{1gx})$	496	496	−496	−496	300	300	−300	−300
$q(t_{1gy})$	496	−496	−496	−496	300	−300	−300	−300
$q(t_{1gz})$	496	496	−496	−496	300	300	−300	−300
$q(t_{2gyz})$	−496	−496	−496	−496	300	300	300	300
$q(t_{2gzx})$	496	−496	−496	−496	300	−300	300	300
$q(t_{2gxy})$	−496	−496	−496	−496	−300	−300	300	300
$q(t_{1u1x})$	300	−300	300	−300	496	−496	−496	496
$q(t_{1u1y})$	300	−300	300	−300	0	0	−496	496
$q(t_{1u1z})$	0	0	300	−300	496	496	−496	496
$q(t_{1u2x})$	701	−701	701	−701	424	−424	−424	424
$q(t_{1u2y})$	701	−701	701	−701	0	0	−424	424
$q(t_{1u2z})$	0	0	701	−701	424	424	−424	424
$q(t_{1u3x})$	0	0	0	0	0	0	0	0
$q(t_{1u3y})$	0	0	0	0	0	−600	0	0
$q(t_{1u3z})$	0	992	0	0	0	0	0	0
$q(t_{2ux})$	0	0	0	0	0	0	0	0
$q(t_{2uy})$	0	0	0	0	−600	0	0	0
$q(t_{2uz})$	992	0	0	0	0	0	0	0

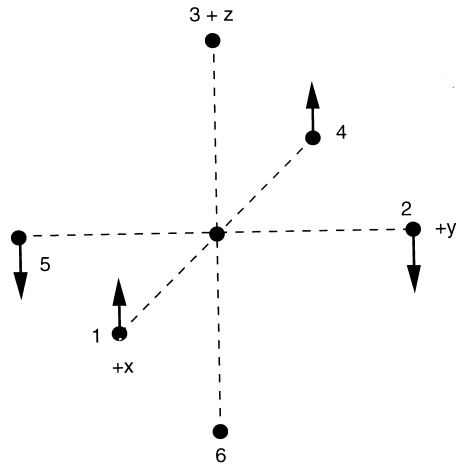

Fig. 2. A typical T_{2u}-distortion mode.

stereochemical lone pair one expects certainly electric dipolar moments. These are present, since these transform in the point group O_h as T_{1u}. There are, however, also rotations (T_{1g}), and distortions of the T_{2g}- and T_{2u}-type.

Since we prefer to keep the discussion as simple as possible, we neglect the charge and will only speak of shifts (T_{1u}) and strain (T_{2g}). Strain, according to Nye (1960) [18] can be described as a symmetrical 3×3 tensor. This can be written in components for the pointgroup O_h as $A_{1g}+E_g+T_{2g}$ of which only the last have appreciable values (Table 5).

Special is the T_{2u}-distortion mode, which is depicted in Fig. 2. It arises only on the digonal type of distorted octahedron, type nr.1 (see Fig. 3 and Table 5). It can be shown to arise from $l=3$ functions, like f-functions. The InCl crystal could be said to have an octupole lattice, since the moments of highest order are of the $l=3$ type. From e.g. Cotton (1971) one finds that $l=3$ functions in octahedral symmetry split into A_{2u}, T_{1u} and T_{2u} functions. We expect also T_{1u} moments from $l=3$ to be present in InCl. However, these are mixed with the shifts, which transform analoguously. Modes of the A_{2u}-type are not present. This

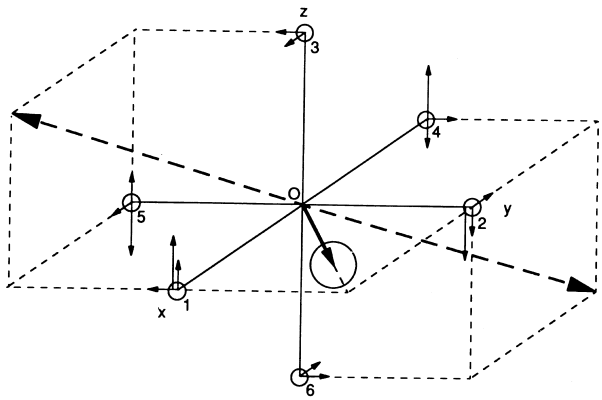

Fig. 3. An In(1)Cl_6 cluster. In order to distinguish the T_{2u} mode from the others, the length of its arrows are shown twice as long.

is because an octahedron has no ligands on the three-fold axes. We will see that another mechanism is present, which causes the point group of the crystal to lower to a tetrahedral point group.

3. Compound distortions

We have seen that the individual octahedra in InCl are severely distorted with several kinds of deformations. In this section we want to discuss compound deformations, since it will be shown that the deformations in InCl are characterized by three types of compound distortions. The first one is chirality, which is well-known and leads to optical rotation of the plane of polarization, and/or to circular dichroism. It can only be present in dissymmetric molecules or complexes, which lack an improper rotation axis, such as inversion or reflection planes or other S_n-axes. The octahedral complexes $InCl_6$ and $ClIn_6$ in InCl are obviously dissymmetric, since at most a three-fold rotation axis is left. One can also form expressions from the distortions given in the previous section, which describe this chirality and therefore should show this dissymmetric character also. Let us denote one of the three types of shift, which transform as T_{1u} by the components μ_x, μ_y and μ_z. And let us denote the components of the rotations (transforming as T_{1g}) as R_x, R_y and R_z. Then the product

$$Hel_1 = \mu_x.R_x + \mu_y.R_y + \mu_z.R_z \quad (1)$$

is a measure for chirality. It looks like a scalar product, but it changes sign under improper rotations. It does not change sign under rotations. It is often called a pseudo-scalar product, because it is not invariant under all symmetry operations (here of the O_h-point group). Fig. 4 shows pictorially how a helix is formed.

These pseudo-scalar products arise for the first time in the fourth order terms of the Landau expansion, since their square is totally symmetric for the symmetry operations of the group.

We pursue this treatment a little further, because it leads to generalizations which are new and which are demonstrated in InCl. Therefore we give in Table 7 only the one-dimensional irreducible representations of the point group O_h:

It is readily shown, that Hel_1 transforms as A_{1u}. For all

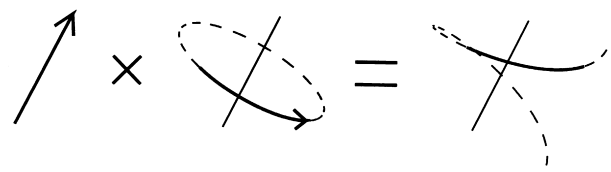

Fig. 4. The combination of a polar and a circular(axial) vector, which form a helix.

Table 7
Character table of the one-dimensional irreducible representations of the point group O_h

O_h	E	$8C_3$	$6C_2$	$6C_4$	$3C_2$	i	$6S_4$	$8S_6$	$3\sigma_h$	$6\sigma_d$
A_{1g}	1	1	1	1	1	1	1	1	1	1
A_{2g}	1	1	−1	−1	1	1	−1	1	1	−1
A_{1u}	1	1	1	1	1	−1	−1	−1	−1	−1
A_{2u}	1	1	−1	−1	1	−1	1	−1	−1	1

improper rotations (or rotoreflections) that are in the right half of the character table, Hel_1 changes sign. Leaving out all operations for which the character is −1 for A_{1u} gives the subgroup O, which is expected to allow optical activity, since it no longer contains improper rotations.

We are used to this type of chirality, since Condon (1937) described the optical activity of chiral molecules, mostly in liquid solvents or in vapours, where the rotation of the plane of polarization depends a.o. on the rotational strength:

$$R_{ba} = Im\langle a|\boldsymbol{p}|b\rangle.\langle b|\boldsymbol{m}|a\rangle \quad (2)$$

Here the (pseudo-) scalar product of an electric ($\langle a|\mathbf{p}|b\rangle$) and a magnetic transition moment ($\langle b|\mathbf{m}|a\rangle$) is present. Regarding the spatial symmetries the rotational strength transforms also like A_{1u}, similar as Hel_1. But a magnetic moment contains dimensionally also the time. This is correct for an electro-magnetic phenomenon such as optical activity, but not for static structures as InCl. In the latter case the magnetic moments are quenched, and we find them again as finite rotations.

There is another contribution, which also transforms as A_{1u}. When one represents the strains as a vector **Q**, with the components Q_{yz}, Q_{zx} and Q_{xy} and when similarly a vector **F** is defined by the T_{2u}-components which transform respectively as $x(y^2-z^2)$, $y(z^2-x^2)$ and $z(x^2-y^2)$, one can show that the pseudo-scalar product **Q**.**F** also belongs to the A_{1u}-representation.

$$Hel_2 = Q_{yz}.F_x + Q_{zx}.F_y + Q_{xy}.F_z \quad (3)$$

This is another source of chirality. It arises because the size of the octahedron is not small with respect to the wave length of the distortion modes. (The edges of the octahedron are approximately one third of the wave length of the Δ-modes). In Fig. 5 we have sketched this new type of chirality. The vectors of the T_{2u}-mode have been replaced by circular currents, as one would expect for the magnetic moments (before quenching). The relevant strains are represented with arrows like electric dipoles. Note that although in each quadrant the direction of the linear arrows and the circular arrows is different, the sign of their product remains the same. In analogy to the rotational strength we would expect here a product of an electric quadrupole transition moment and a magnetic quadrupole transition moment.

We are here beyond the Condon (1937) approximation, which seems quite sufficient for the treatment of circular dichroism and optical rotatory power of ordinary light, where in general the wave length of the light is large with respect to the size of the molecules or complexes. However, even in the Condon theory it is not correct to neglect the size of a molecule with respect to the wave length of the light used. Hel_2 describes an additional term in the expansion, which is not small as can be seen in Table 5.

In Table 8 we give an illustration of these helical modes on two neighbouring columns of ions, subject to a single $\mathbf{k}_6$-mode and its complex conjugate. This mode represents a planar wave along the z-direction. ($\mathbf{k}_6^1 = \pi(0,0,1)/a_0$, where a_0 is the cubic B1 axis.) For each of these ions the columns give their position, their displacements (in the 'geometric' approximation), and finally all moments of the octahedron for which they form the center. One can check that a quantity like $\mu 1_x.R_x + \mu 1_y.R_y$ is equal for the two columns. Instead of $\mu 1$ we might have used $\mu 2$ or $\mu 3$, since these are equivalent in a group theoretical sense. Similarly $Q_{yz}.F_x + Q_{zx}.F_y$ is equal for the neighbouring columns. Eqs. (1) and (3) give in addition a third product. These arise only properly when also the $\mathbf{k}_6$-modes travelling along the x- and the y-direction are included. It can be proven [14] that the lattice modes with the $\mathbf{k}_6$ wave vectors induce a ferrodistortive chirality.

In InCl the procedure just followed can be generalized for other compound distortions. These compound deformations are not so famous as helices, since a corresponding

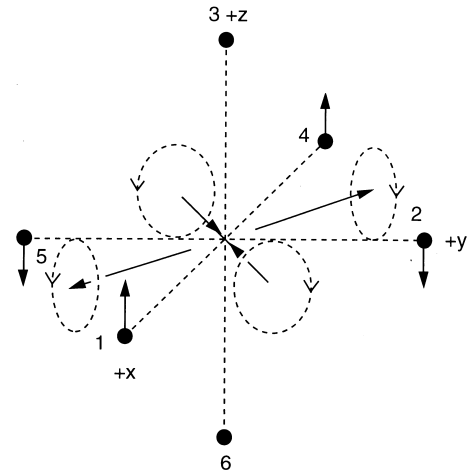

Fig. 5. A new type of chirality represented by circular (axial)vectors from a dynamic T_{2uz} moment. Note that the sense of the helices are the same for the four quadrants.

Table 8
The distortion by the $\mathbf{k}_6^1$-mode of two columns of ions. The numbers are fractions $\times 10^4$ of the InCl cell parameter

	$In3_1$	$Cl2_3$	$In4_2$	$Cl2_3$		$Cl1_1$	$In1_3$	$Cl1_{10}$	$In1_{12}$
Position					Position				
x	0	0	0	0	x	2500	2500	2500	2500
y	0	0	0	0	y	0	0	0	0
z	0	2500	5000	7500	z	0	2500	5000	7500
Shifts					Shifts				
dx	150	0	−150	0	dx	248	0	−248	0
dy	0	−248	0	248	dy	0	−150	0	150
dz	0	0	0	0	dz	0	0	0	0
Moments					Moments				
R_x	248	0	−248	0	R_x	150	0	−150	0
R_y	0	−150	0	150	R_y	0	−248	0	248
R_z	0	0	0	0	R_z	0	0	0	0
Q_{yz}	−248	0	248	0	Q_{yz}	−150	0	150	0
Q_{zx}	0	−150	0	150	Q_{zx}	0	−248	0	248
Q_{xy}	0	0	0	0	Q_{xy}	0	0	0	0
$\mu 1_x$	150	0	−150	0	$\mu 1_x$	248	0	−248	0
$\mu 1_y$	0	−248	0	248	$\mu 1_y$	0	−150	0	150
$\mu 1_z$	0	0	0	0	$\mu 1_z$	0	0	0	0
$\mu 2_x$	350	0	−350	0	$\mu 2_x$	212	0	−212	0
$\mu 2y$	0	−212	0	212	$\mu 2_y$	0	−350	0	350
$\mu 2_z$	0	0	0	0	$\mu 2_z$	0	0	0	0
$\mu 3_x$	248	0	−248	0	$\mu 3_x$	150	0	−150	0
$\mu 3_y$	0	−150	0	150	$\mu 3_y$	0	−248	0	248
$\mu 3_z$	0	0	0	0	$\mu 3_z$	0	0	0	0
F_x	248	0	−248	0	F_x	150	0	−150	0
F_y	0	150	0	−150	F_y	0	248	0	−248
F_z	0	0	0	0	F_z	0	0	0	0

phenomenon such as optical activity is lacking. Suppose we have a quantity that belongs to an A_{2u} representation. That can only exist when all symmetry operations which have a character -1 for A_{2u} are taken away. Starting from the original O_h point group symmetry, we arrive at T_d. In other words there is tetrahedron forming. Since we already discussed the formation of helices, we can see from Table 7 that only the point group T is left, if we cut all symmetry elements for which the character is -1 either from A_{1u} or A_{2u}.

The following pseudo-scalar product between shifts and strains belongs to A_{2u}:

$$Tetr_1 = \mu_x.Q_{yz} + \mu_y.Q_{zx} + \mu z.Q_{xy}$$

This expression is easily explained, since it behaves as *xyz* and has therefore plus and minus signs on the corners of a cube (Fig. 6).

The trigonally distorted octahedrons, point along three-fold axes to the corners of the cubic cell. One could imagine that all eight corner-directions of the cube were equally used, so that the cubic symmetry would again be restored. This, however, is not the case in InCl, where there are 20 trigonally distorted octahedra in a cell. Since 20 is not divisible by 8 cubic symmetry cannot exist. A tetrahedral symmetry can, however.

We note that a second contribution to the A_{2u} irreducible representation is formed by:

$$Tetr_2 = R_x.F_x + R_y.F_y + R_z.F_z \quad (5)$$

Table 9 displays the moments of two neighbouring columns for the $\mathbf{k}_8^1$-mode ($\mathbf{k}_8^1 = \pi(2,0,1)/a_0$). This is also a circularly polarized mode, but the helical sense of two neighbouring columns is opposite. This corresponds with the formation of an antiferrodistortive ordering of chirality by these modes [14]. The tetrahedral expressions $Tetr_1$ and $Tetr_2$ give the same value for the two columns. This indicates that the $\mathbf{k}_8$-modes induce the ferrodistortive tetrahedron character, which can be proven [14].

A third compound distortion transforms as A_{2g}. The

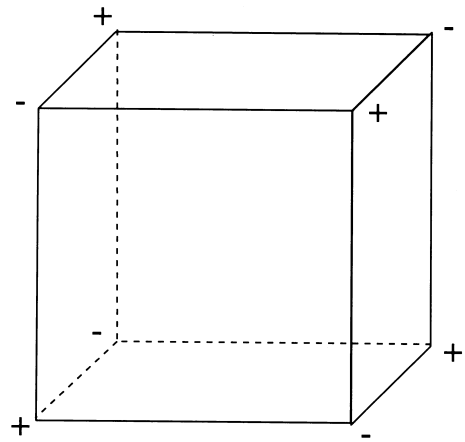

Fig. 6. A cube showing the symmetry of *xyz* (A_{2g}).

Table 9
The distortion by the $\mathbf{k}_8^1$-mode of two columns of ions. The numbers are fractions $\times 10^4$ of the InCl cell parameter

	$In3_1$	$Cl2_3$	$In4_2$	$Cl2_3$		Cl_1	$In1_3$	$Cl1_{10}$	$In1_{12}$
Position					Position				
x	0	0	0	0	x	2500	2500	2500	2500
y	0	0	0	0	y	0	0	0	0
z	0	2500	5000	7500	z	0	2500	5000	7500
Shifts					Shifts				
dx	150	0	−150	0	dx	248	0	−248	0
dy	0	248	0	−248	dy	0	−150	0	150
dz	0	0	0	0	dz	0	0	0	0
R_x	−248	0	248	0	R_x	150	0	−150	0
R_y	0	−150	0	150	R_y	0	−248	0	248
R_z	0	0	0	0	R_z	0	0	0	0
Q_{yz}	248	0	−248	0	Q_{yz}	−150	0	150	0
Q_{zx}	0	−150	0	150	Q_{zx}	0	−248	0	248
Q_{xy}	0	0	0	0	Q_{xy}	0	0	0	0
$\mu 1_x$	150	0	−150	0	$\mu 1x$	248	0	−248	0
$\mu 1_y$	0	248	0	−248	$\mu 1_y$	0	−150	0	150
$\mu 1_z$	0	0	0	0	$\mu 1_z$	0	0	0	0
$\mu 2_x$	350	0	−350	0	$\mu 2_x$	212	0	−212	0
$\mu 2_y$	0	212	0	−212	$\mu 2_y$	0	−350	0	350
$\mu 2_z$	0	0	0	0	$\mu 2_z$	0	0	0	0
$\mu 3_x$	−248	0	248	0	$\mu 3_x$	−150	0	150	0
$\mu 3_y$	0	−150	0	150	$\mu 3_y$	0	248	0	−248
$\mu 3_z$	0	0	0	0	$\mu 3_z$	0	0	0	0
F_x	−248	0	248	0	F_x	−150	0	150	0
F_y	0	150	0	−150	F_y	0	−248	0	248
F_z	0	0	0	0	F_z	0	0	0	0

reduction of the point group of the crystal from O_h could be imagined by combining an object transforming as A_{2g} and helices or tetrahedrons. We named these spirals and a quantity that transforms as a spiral (A_{2g}) is:

$$Spir_1 = R_x.Q_{yz} + R_y.Q_{zx} + R_z.Q_{xy} \quad (6)$$

One expects also a second form:

$$Spir_2 = \mu_x.F_x + \mu_y.F_y + \mu_z.F_z \quad (7)$$

Especially $Spir_1$ is demonstrated clearly in the structure. Characteristic is half the swastika which is decomposable in a rotation and a strain (Fig. 7). Their product taken over all directions is equal to $Spir_1$. For the geometric approximation, an antiferrodistortive type of ordering is found. The contribution from $Spir_2$ happens to be zero for the geometric approximation. It is not zero for e.g. only the Δ-waves.

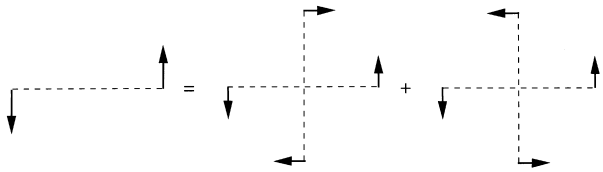

Fig. 7. The decomposition of the 'spiral' compound mode into a strain (T_{2g}) and a rotation (T_{1g}). Their product represents a part of the bilinear product, which transforms as A_{2g}.

4. The lattice modes

The modes which form the geometric approximation have been denoted in [14] by the $\mathbf{k}_6$, the $\mathbf{k}_8$ and the $\mathbf{k}_4$ vectors. In Fig. 8 we picture the displacements of the ions due to the $\mathbf{k}_6$ vectors travelling in the z-direction. These look similar to transversal planar waves. The amplitudes for the In- and the Cl-ions differ as has to be expected. But their helical displacements are a result of their circular polarization. There are similar helices for the x- and the y-direction. These $\mathbf{k}_6$-waves give the ferrodistortive chirality of InCl, since the senses of these helices along the z-direction are all the same. In^+-ions are represented by the smaller circles. $Cl^-$are represented by the larger circles. The different types of ion have been indicated with black quarters, which are numbered as the quarters of an hour. The difference between the four types shows only when different kinds of waves are superimposed on each other.

Characteristic for of the three types of modes is that rows of ions are shifted longitudinally and dimerized. This dimerization helps to make space for the lone pairs. The difference between the three modes is due to their transversal behaviour. For the $\mathbf{k}_6$ neighbouring rows shift in a parallel way.

The displacements due to the $\mathbf{k}_8$-modes, which travel in the z-direction are shown in Fig. 9. These are also helical, however, neighbouring columns differ in sense. Therefore, this does not lead to ferrodistortive chirality. One can show

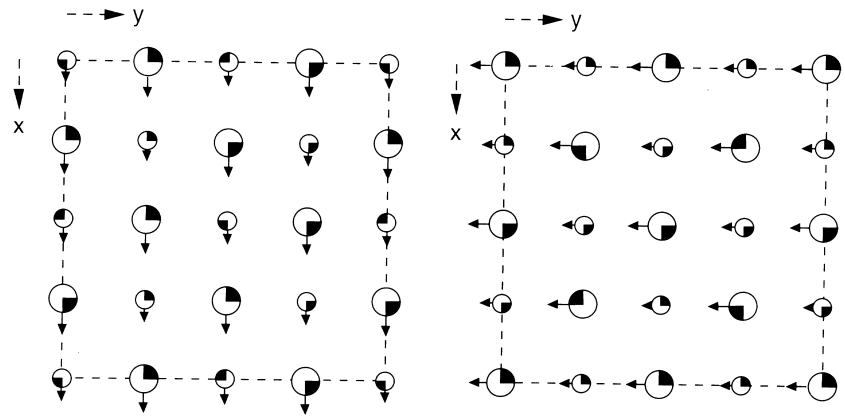

Fig. 8. $\mathbf{k}_6^1$ for $z=0$ (left) and $z=1/4$ (right). In^+ (Cl^-) ions are represented by small (large) circles. The types of ion (1, 2, 3, or 4) are denoted like the quarters of an hour.

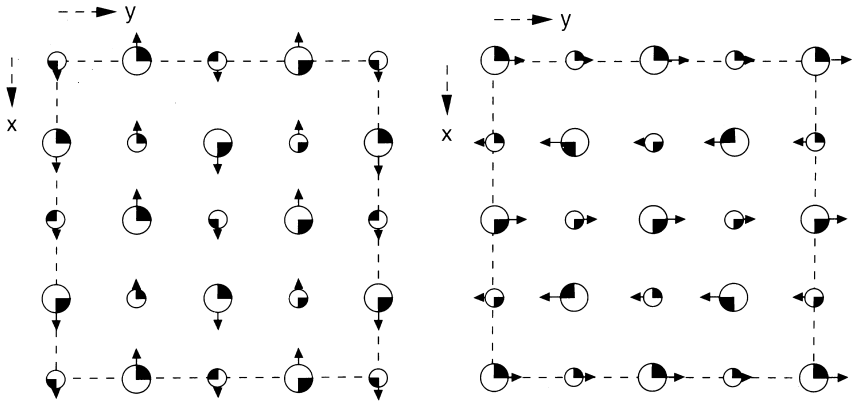

Fig. 9. $\mathbf{k}_8^1$ for $z=0$ (left) and $z=1/4$ (right). The ion notation is the same as that for Fig. 8.

that an antiferrodistortive pattern of chirality is formed. These waves appear to produce a ferrodistortive arrangement of tetrahedral deformations like in Fig. 6.

The longitudinal pattern from the $\mathbf{k}_8$ modes is similar as for the $\mathbf{k}_6$ modes. However, neighbouring rows are now shifted in the opposite direction.

We studied also what happens when these $\mathbf{k}_6$ and $\mathbf{k}_8$ waves are combined (Fig. 10). Especially in the geometric

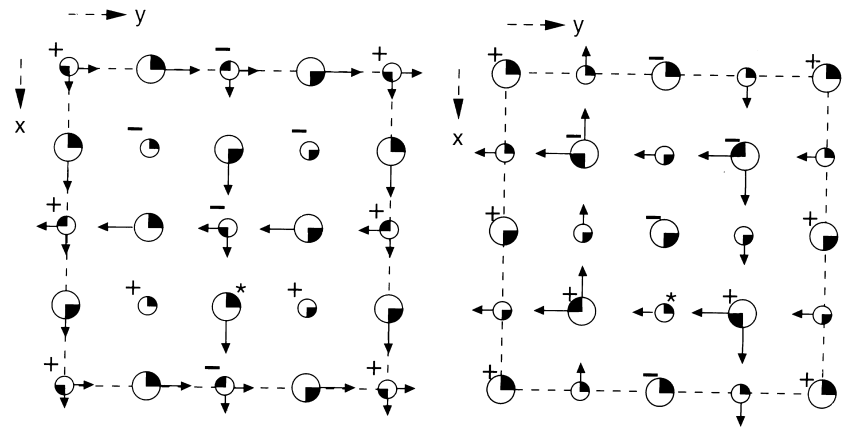

Fig. 10. The complete $\mathbf{k}_6$- and $\mathbf{k}_8$-modes for $z=0$ (left) and $z=1/4$ (right). The asterix denotes a column of type 1 ions, which have parallel T_{2u}-modes.

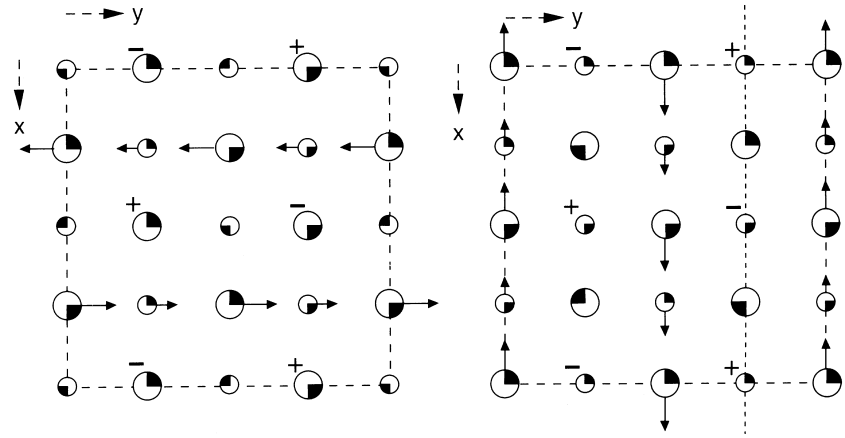

Fig. 11. The *x*-, *y*-, *z*-components of the displacements of the $\mathbf{k}_4$-modes for $z=0$ (left) and $z=1/4$ (right). The dotted line denotes ions with even modes (see Fig. 7).

approximation, since their amplitudes are equal in absolute sense, these waves reinforce or annihilate each other. The different types of ion are formed. The total chirality appears to be conserved, as we could check with a computer, but the contribution of the local sites differs. This phenomenon is called interference. Fig. 10 shows this for $z=0$ and $z=1/4$. The asterisk denotes two type 1 ions, which form a column with T_{2u}-deformations. Notice how through the shifts of rows the type 1 anions and cations naturally fit together.

In Fig. 11 we show the displacements due to $\mathbf{k}_4$ modes. These are special since these introduce the spirals. A series of these forms have been indicated by a dotted line for $z=1/4$. Note that these fill part of the gaps left open by the interference of the $\mathbf{k}_6$ and $\mathbf{k}_8$-modes (Fig. 10). The longitudinal pattern of the $\mathbf{k}_4$ modes is similar as for the other modes. However, neighbouring rows are not shifted at all. We expect that the dimerization requires most of the energy and that since these modes do not differ in this respect these are practically degenerate.

One can show that the spirals have an antiferrodistortive arrangement for the $\mathbf{k}_4$ vectors. For example, in Fig. 11 at the right along the dotted line, the spirals have the same sign as those in the same square on the left. This is because both the rotation and the strain change sign. On the other hand on the square at the left of this figure either the rotation or the strain has changed sign and therefore the $Spir_1$ has an opposite value for these planes.

Figs. 12 and 13 give the combination of these three modes and consequently represent the ‘geometric’ approximation.

As has been shown, the distortions can be described as line displacements of rows of ions. In the ‘geometric’ approximation it turns out that only 3/4 of all line displacements are present. The space group, however, has then already been reduced to $P2_13$. But one can show that the type 2 $InCl_6$ octahedra are not trigonally distorted yet. By comparing the real structure and the approximate one, it appears that the extra distortions change the type 2 $InCl_6$ and $ClIn_6$ into ‘almost’ trigonal ones. The digonally distorted octahedra, however, keep their characteristic shape (Fig. 1).

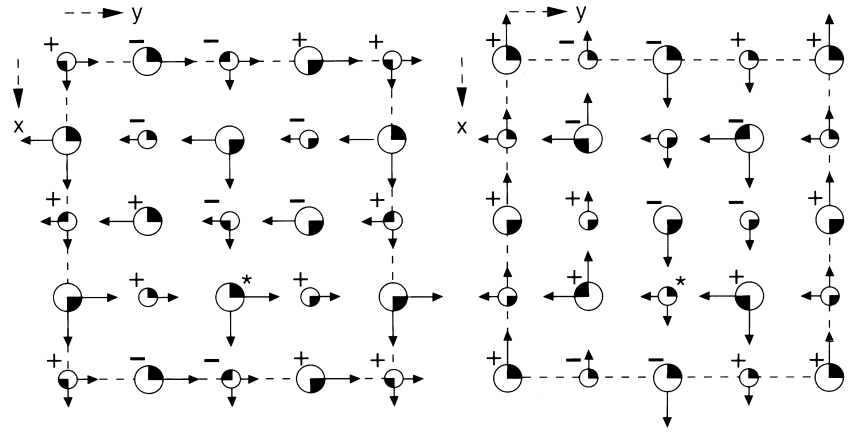

Fig. 12. InCl in the ‘geometric’ approximation; $z=0$ (left) and $z=1/4$ (right).

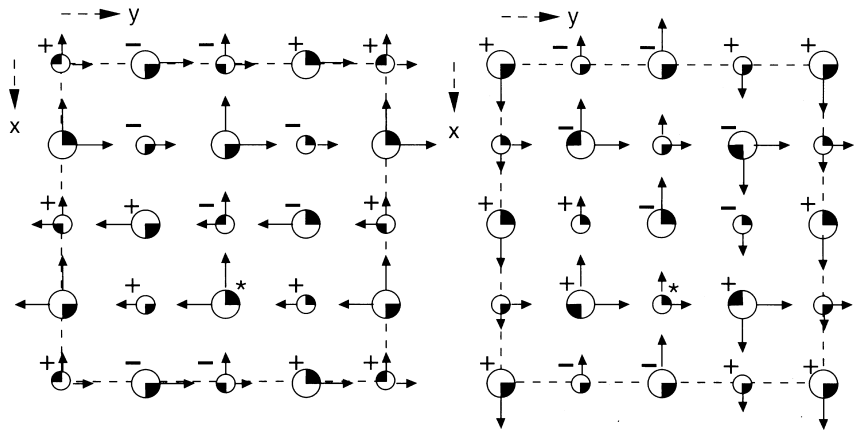

Fig. 13. InCl in the 'geometric' approximation; $z=1/2$ (left) and $z=3/4$ (right).

5. Discussion

Summarizing, we have described the cooperative Jahn–Teller effect of two types of $InCl_6$-octahedra, which exhibit stereochemical activity of the lone pairs arising from the ($5s^2$) outer electron configuration of the In^+-ions. That this is due to pseudo-Jahn–Teller effects and Jahn–Teller effects has been established previously ([9,10]).

We have started with the local description of the distortions of the octahedra, which are regular in the undistorted B1 structure. This method has developed in our group. It can be used when evidence is available for distortions of more symmetric complexes. In the case of yellow InCl, its space group is a subgroup of the group of rocksalt. There are also no space groups in between $P2_13(T^4)$ and $F\bar{3}m$ ($O_h{}^5$), which could have been chosen. The distortions due to $\mathbf{k}_6$ and $\mathbf{k}_8$ lead directly to the space group of InCl. The relatively large number of local modes needed to describe the distortions is surprising.

Rather than describing all arrangements of the primary moments of distortion, we studied the compound distortions. There are three types. The helices, the tetrahedrons and the spirals. These descriptions are original, although helical distortions are more known from the theory of optical rotation (see e.g. Kauzmann [19]). The static helices in InCl can be related to the description of the optical rotation strength, which is a product of an electric and a magnetic transition moment (Condon [17]). We have to consider in the static structure the magnetic moment as quenched, which means that the magnetic moment is replaced by a finite rotation. The time is left out and the spatial behaviour of the rotation and the magnetic moment are similar (both behave as axial vectors, see e.g. Nye [18] for the definition of 'axial' vectors). The pseudo-scalar product of shifts and rotations gives then the measurable quantity Hel_1. It changes sign for all improper rotations (rotoreflections) like the optical rotation strength.

There is, however, a second form, which transforms similarly. It is the pseudo-scalar product of strain times T_{2u}-components. It is due to the fact that the octahedrons' dimensions are not small with respect to the wave length of the helix. When one could go back from the static case in InCl to the dynamic case for light, one would be able to deduce an additional optical rotation strength proportional to:

$$\langle a|\mathbf{Q}_e|b\rangle\langle b|.\mathbf{Q}_m|a\rangle \tag{8}$$

Here the product of a transition moment of an electric quadrupole and a magnetic quadrupole are given. ($\mathbf{Q}_e$ is restricted to its T_{2g}-subset.) In Fig. 5 we have sketched these. This goes beyond the Condon [17] approximation, which is particularly able for the description of the optical rotation of small molecules. We are not aware of rotational strength of this quadrupolar type, for e.g. liquid crystals, where the size of these molecules *is* often of the order of the wave length of light (e.g. [20]).

The $\mathbf{k}_6$ modes cause the ferrodistortive chirality. The $\mathbf{k}_8$-modes and the $\mathbf{k}_4$-modes induce antiferrodistortive arrangements of chirality. Due to interference of these modes, there is a lot of reshuffling. But the total chirality, calculated by Hel_1 or/and Hel_2 remains the same when summed over all sites, as we found out by calculation. In particular the difference between the octahedra of type 1 and the others is a result of this interference. This applies to the $InCl_6$ as well as the $ClIn_6$ octahedra of type 1. It is only the ferrodistortive chirality that is expected to be measurable by optical polarimetry or circular dichroism.

The two other compound distortions are not so well-known, since these have no corresponding optical applications. We are unaware of earlier descriptions of these. We have established in Section 2, that individual octahedrons never show tetrahedrons. Because there are no ligands on the three-fold axes, there are no A_{2u}-distortions. Therefore the resulting tetrahedral symmetry of the crystal has to come from the compound distortion, which transforms as A_{2u}.

As we have seen, the space group of yellow InCl is a

subgroup of the space group of NaCl. This means that the first condition for continuous phase transitions according to Landau and Lifshitz [13] has been fulfilled. We have discussed also the second condition.

The third condition for a second order phase transition is that no third order anharmonic term should be present. It can be proved, however, that the three modes of different irreducible representations together give a third order invariant [14]. And also that this can be traced back to the anharmonic energy term of the digonally distorted octahedron [10] (see Fig. 3). In the hypothetical case of a phase transition to the rocksalt structure this condition would have been proof of a first order phase transition. Also, when having three modes belonging to different irreducible representations, one expects energy terms which are a consequence of their coexistence. The third order invariant is the first term of the expansion of the free energy, that accomplishes this. Obviously the third order anharmonic energy term of the type 1 $InCl_6$ octahedron is of pivotal significance for this structure.

There are numerous fourth order invariants. These can be derived a.o. by squaring the pseudo-scalar terms. They correspond to fourth order anharmonic energy contributions, which have not been written down in this paper. In principle more terms of the Landau expansion could be given, but since no corresponding phase transition has been found we will not do so. In general one needs a fourth order or a sixth order anharmonic energy term, in order to keep the orderparameter bounded (e.g. Kittel [21]).

There is also the fourth Landau condition, which is about the stability versus incommensurate structures. However, InCl has a commensurate structure. We refer to [14] for further discussions.

Appendix A

The distortion modes of an octahedral complex with point group O_h are given in Table 10. There is only one coordinate system. It is at the centre of the (idealized) octahedron. This coordinate system is right-handed. The central ion is labeled 0. The ligands on the positive x, y and z-axis are labeled 1,2,3 and on the negative side 4,5 and 6 respectively (Van Vleck [16] convention). Shifts from the ideal octahedron positions are denoted as e.g. x_4, y_4 and z_4 for the ion with the idealized position at the negative x-axis. There are three types of three-fold degenerate T_{1u}-modes, which are chosen orthogonal. In practice these will mix.

Table 10
Symmetry modes of an octahedron

$q(a_{1g})$	$(x_1+y_2+z_3-x_4-y_5-z_6)/\sqrt{6}$
$q(e_{g\theta})$	$(2z_3-x_1-y_2-2z_6+x_4+y_5)/\sqrt{12}$
$q(e_{g\epsilon})$	$(x_1-y_2-x_4+y_5)/2$
$q(t_{1gx})$	$(z_2-y_3-z_5+y_6)/2$
$q(t_{1gy})$	$(x_3-z_1-x_6+z_4)/2$
$q(t_{1gz})$	$(y_1-x_2-y_4+x_5)/2$
$q(t_{2gyx})$	$(z_2+y_3-z_5-y_6)/2$
$q(t_{2gzx})$	$(x_3+z_1-x_6-z_4)/2$
$q(t_{2gxy})$	$(y_1+x_2-y_4-x_5)/2$
$q(t_{1u1x})$	x_0
$q(t_{1u1x})$	y_0
$q(t_{1u1x})$	z_0
$q(t_{1u2x})$	$(x_1+x_4)/\sqrt{2}$
$q(t_{1u2y})$	$(y_2+y_5)/\sqrt{2}$
$q(t_{1u2z})$	$(z_3+z_6)/\sqrt{2}$
$q(t_{1u3x})$	$(x_2+x_3+x_5+x_6)/2$
$q(t_{1u3y})$	$(y_1+y_3+y_4+y_6)/2$
$q(t_{1u3z})$	$(z_1+z_2+z_4+z_5)/2$
$q(t_{2ux})$	$(x_2-x_3+x_5-x_6)/2$
$q(t_{2uy})$	$(y_3-y_1+y_6-y_4)/2$
$q(t_{2uz})$	$(z_1-z_2+z_4-z_5)/2$

References

[1] J.M. Van den Berg, Thesis, Leiden University, 1964.
[2] J.M. Van den Berg, Acta Crystallogr. 20 (1966) 905–910.
[3] C.P.J.M. Van der Vorst, G.C. Verschoor, W.J.A. Maaskant, Acta Crystallogr. B 34 (1980) 3333–3335.
[4] C.P.J.M. Van der Vorst, W.J.A. Maaskant, J. Solid State Chem. 34 (1980) 301–313.
[5] C.P.J.M. Van der Vorst, J. Phys. Chem. Solids 42 (1981) 655–665.
[6] U. Öpik, M.H.L. Pryce, Proc. Roy. Soc. (London) A238 (1957) 425–447.
[7] F.S. Ham, Phys. Rev. B 8 (1973) 2926–2944.
[8] R.G. Pearson, Symmetry Rules for Chemical Reactions, Wiley, New York, 1976.
[9] W.J.A. Maaskant, I.B. Bersuker, J. Phys. Condens. Matter 3 (1991) 37–47.
[10] W.J.A. Maaskant, New J. Chem. 17 (1993) 97–105.
[11] L.D. Landau, Sov. Phys.-JETP 7 (1937) 627.
[12] L.D. Landau, Phys. Z. Sowjetunion 11 (1937) 545–555.
[13] L.D. Landau, E.M. Lifshitz, Statistical Physics, 3rd ed., part 1, Pergamon, Oxford, 1980.
[14] W.J.A. Maaskant, J. Phys. Condens. Matter 9 (1997) 9759–9783.
[15] F.A. Cotton, Chemical Application of Group Theory, 2nd ed., Wiley-Interscience, New York, 1971.
[16] J.H. Van Vleck, J. Chem. Phys. 7 (1939) 72–84.
[17] E.U. Condon, Rev. Mod. Phys. 9 (1937) 431–457.
[18] J.F. Nye, Physical Properties of Crystals, Clarendon Press, Oxford, 1960.
[19] W. Kauzmann, Quantum Chemistry, Academic Press, New York, 1957.
[20] S.F. Mason, Molecular Optical Activity and the Chiral Discriminations, Cambridge University Press, Cambridge, 1982.
[21] C. Kittel, Introduction to Solid State Physics, 5th ed., Wiley, New York, 1976.